Journal of Metals, Materials and Minerals, Vol.29 No.2 pp.87-97, 2019

Wood plastic composites based on recycled poly(ethylene terephthalate) and poly(butylene adipate-*co*-terephthalate)

Phasawat CHAIWUTTHINAN[1,*], Aphichat PIMPONG[2], Amnouy LARPKASEMSUK[3], Saowaroj CHUAYJULJIT[4] and Anyaporn BOONMAHITTHISUD[4]

[1]*MTEC, National Science and Technology Development Agency (NSTDA), Thailand Science Park, Khlong Luang, Pathum Thani, 12120, Thailand*
[2]*Department of Petrochemical and Polymer Science, Faculty of Science, Chulalongkorn University, Pathumwan, Bangkok, 10330, Thailand*
[3]*Department of Materials and Metallurgical Engineering, Faculty of Engineering, Rajamangala University of Technology Thanyaburi, Pathum Thani, 12110, Thailand*
[4]*Department of Materials Science, Faculty of Science, Chulalongkorn University, Pathumwan, Bangkok, 10330, Thailand*

[*]**Corresponding author e-mail:** phasawc@metec.or.th

Received date:
14 September 2018
Revised date:
3 December 2018
Accepted date:
11 January 2019

Keywords:
WPCs
Recycled PET
Poly(butylene adipate-co-terephthalate)
Wood flour
Mechanical and thermal properties
Morphology

Abstract

In this work, wood plastic composites (WPCs) were prepared from a selected recycled poly(ethylene terephthalate) (rPET)/poly(butylene adipate-co-terephthalate) (PBAT) blend ratio. The 70/30 (wt%/wt%) (rPET)/PBAT blend was incorporated with six loadings of wood flour (WF) (5–30 wt%) through melt mixing on a twin screw extruder, followed by injection molding. The mechanical properties of the WPCs, in terms of the impact, tensile and flexural strength, Young's modulus and elongation at break were determined as a function of the WF content. The results showed that the impact strength and elongation at break of the WPCs were all lower than those of the neat blend. However, the WPCs at 5–15 wt% WF and all had higher impact strength and elongation at break than the neat rPET, respectively. In contrast, the tensile strength of all the WPCs was much lower than that of the neat rPET, and only at high WF content (20–30 wt%) exhibited higher tensile strength than the neat blend. In addition, the Young's modulus and flexural strength of the WPCs were all higher than those of the neat blend. However, the WPCs at 5 and 10 wt% WF had lower Young's modulus than the neat rPET, while all the WPCs had lower flexural strength than the neat rPET. Moreover, the WF acted as a nucleating agent, which consequently gave rise to the increased crystallization temperature, degree of crystallinity and melting temperature of the rPET component in WPCs, as revealed by the differential scanning calorimetry. However, thermogravimetric analysis showed a decrease in the thermal stability of the rPET/PBAT blend upon addition of WF. Meanwhile, all the WPCs exhibited an enhanced water uptake over the neat blend (up to 5.7-fold at 30 wt% WF).

1. Introduction

Recently, there has been a growing interest in wood-plastic composites (WPCs) and their applications. WPCs are mainly a combination of plastics (matrix) and wood (reinforcement), which provide properties superior to individual component. WPCs can be made from virgin plastics and/or recycled ones [1-3]. This study aimed at the use of both recycled plastic, i.e., recycled poly(ethylene terephthalate) (rPET) as a major phase and virgin biodegradable plastic, i.e., poly(butylene adipate-*co*-terephthalate) (PBAT) as a minor one, and wood flour (WF), which is mainly due to the environmental awareness and the saving petroleum resources and cost. Nowadays, both rPET and WF are commercially available, abundant and cheap. This is because the use of PET over the world is increasing daily as synthetic fibers, packaging films and soft drink bottles owing to its several unique properties such as good mechanical properties, transparency, light weight, high thermal stability, excellent chemical resistance and barrier properties, non-toxic and recyclability [4-12]. Moreover, it can be last long after the end of life without significant loss of its physical properties, according to its extremely resistant to hydrolysis, bacterial and fungal attack in the environment [7,8,13-19]. Most of the postconsumer PET bottles are usually used only once and then discarded into the environment, which inevitably create a large amount of PET waste. Mechanical recycling of PET wastes is an economical and effective way for the partial solving of the existing environmental problem and the conservation of raw petrochemical products and energy. Thus, PET bottles become one of the most valuable and successfully recyclable plastics because of their easy sorting, collection and recovery from municipal solid wastes and also fully recyclable. However, the physical properties of rPET

DOI: 10.14456/jmmm.2019.23

products such as toughness, moldability, thermal stability and notched impact strength are dropped mainly by the thermal, hydrolytic and mechanical degradations during melt processing, which in turn limit its applications [10,11,20]. To recover the performance of rPET, various methods have been attempted to modify PET waste into new value-added raw materials with a wider range of properties. These include reinforcement, blending and filling with other materials. In general, melt mixing of rPET with highly flexible plastics is a straightforward and relatively simple method to improve the toughness, impact strength and melt processability of the rPET [5,9,12]. The flexible plastic used in this work was PBAT, which is a biodegradable aliphatic-aromatic thermoplastic copolyester with interesting properties such as high toughness, melt processability, good thermal stability and no adverse effect on the environment. PBAT can be degraded into basic monomers (1.4-butanediol, terephthalic acid and adipic acid) and eventually to carbon dioxide, water and biomass through the metabolism of biological enzymes or microorganisms existing in soil or compost. Because PBAT contains many hydrolyzable units (butylene adipate) in the main chain, it can be fully biodegraded within a few weeks, and thus modifies biodegradability of rPET products after discarding. In addition, the aromatic units (butylene terephthalate) in PBAT offer an optimal balance between biodegradability and physical properties, which may be developed for both structural and non-structural applications [17-19]. Thus, blending rPET with PBAT may yield a combination of the desired properties of each component, and form a potential matrix for preparing composites with WF to create new materials with tailored properties and performances. WF is now gaining increasing interests because of its low cost, light weight, renewability, abundance, recyclability and biodegradability [4,7,13,21-23]. Hence, WF can help resolving environmental issues and also has an economic advantage over synthetic fibers. WF has been used worldwide in the preparation of WPCs with different thermoplastics and thermoset plastics, due to its low cost and abrasion to processing equipment, high aspect ratio (length/diameter, L/D), abundant availability, renewability, acceptable specific strength, biodegradability and non-toxic characteristics [4,8,18,19,21]. WPCs can be fabricated into products using conventional plastic processing techniques such as extrusion, compression molding and injection molding for using in structural and automotive industries. Many previous works have reported that either recycled thermoplastic or biodegradable plastic has been recently considered for producing WPCs [23-27]. Nowadays, commercial WPCs have already been used since they can be sawed, screwed and nailed using conventional tools like wood materials. However, to the best of our knowledge, there has been no study on the characteristics of the WPCs based on the rPET and PBAT.

In this study, a series of rPET/PBAT/WF composites were prepared in order to tailor their properties, extend their applications and reduce the overall material cost. With this respect, the mechanical properties (impact, tensile and flexural tests), thermal properties (differential scanning calorimetry (DSC) and thermogravimetric analysis (TGA), morphology (scanning electron microscopy (SEM)) and water uptake of the resulting products were then comparatively investigated.

2. Experimental

2.1 Materials

The rPET chips were mainly obtained from scrap of postconsumer bottles. PBAT (Ecoflex® F Blend C1200, BASF, Germany) with a density of 1.25-1.27 g·cm^{-3}, a melt flow rate of 2.7-4.9 g/10 min (190°C/2.16 kg), a glass transition temperature (T_g) of -30°C and a DSC melting temperature (T_m) in the range of 110-120°C, was obtained from BASF The Chemical Company (Germany). WF (Lignocel C120) with a bulk density and grain size of 1-1.35 g·cm^{-3} and 70-150 μm, respectively, was supplied by J. Retenmaier & Sohne Co. (Germany). All materials were used as received without further purification.

2.2 Sample preparation

Prior to mixing, the rPET chips, PBAT pellets and WF powder were oven-dried at about 100, 65 and 100°C, respectively for 48 h to remove any trace of moisture. First, the rPET was melt mixed with different loadings of PBAT (0, 10, 20, 30, 40 and 50 wt%) on a twin-screw extruder (Lab Tech Engineering LW-100, Thailand) operated at a temperature profile of 240, 240, 235, 235, 230, 230, 230 and 225°C from the feed zone to the die head at a fixed screw rotational speed of 65 r m^{-1}. The extrudates were pelletized and then injection molded into the standard test specimens using an injection molding machine (Battenfield BA 250 CDC, UK) at 235-250°C. The rPET/PBAT/WF composites were also prepared from a selected rPET/PBAT blend as above with the addition of six different loadings of WF (5, 10, 15, 20, 25 and 30 wt%). The PBAT standard test specimens were also prepared using the same injection molding machine, but at 120°C.

2.3 Characterization

The Izod impact test was conducted on a notched impact specimen using an impact tester (Ceast, Resil Impactor 10K, USA), according to the ASTM D256 standard with a sample size of 6.35 × 1.27 × 3 mm^3. The tensile test was performed with a dumbbell-shaped specimen on a universal testing machine (Instron 5500R, USA), according to the ASTM D638 standard with a load cell capacity of 10 kN and a crosshead speed of 50 mm min^{-1}. The flexural test was performed under three-point bending on a rectangular-shaped specimen using a universal testing machine (Lloyd 500, UK), according to the ASTM D790 standard with a load cell capacity of 2.5 kN and a

crosshead speed of 15 mm min^{-1}. The values of all the mechanical properties were averaged from at least five specimens.

The morphology of WF particles and fractured surface of the impact sample was analyzed by scanning electron microscopy (SEM; Jeol JSM-5410LV microscope, Japan) at an accelerated voltage of 10 kV and 15 kV and a magnification of ×100 and ×1,000, respectively. The fractured surface of the sample was sputter coated with a thin layer of gold under vacuum to avoid electrostatic charge buildup during examination.

The thermal behaviors of the samples were determined by DSC (Netzsch 204 F1 Phoeni, Germany) under a nitrogen (N_2) atmosphere at a gas flow rate of 50 mL min^{-1}. The sample was heated from 30°C to 300°C (first heating run) and held isothermally for 5 min to erase its previous thermal history. Then, the sample was cooled to 30°C (cooling run) and subsequently reheated to 300°C (second heating run) and finally cooled down to room temperature (RT). All measurements were conducted at the same heating/cooling rate of 10°C min^{-1}. The thermograms obtained from the cooling and second heating runs provided crystallization temperature (T_c) and melting temperature (T_m) while the degree of crystallinity (χ_c) of the rPET phase was calculated by a heat of fusion (ΔH_m) taken from the area of melting endothermic peak using Eq. (1),

$$\chi_c\ (\%) = [\Delta H_m/\Delta H^\circ_m w] \times 100 \qquad (1)$$

where ΔH^o_m is the heat of fusion for 100% crystalline rPET with a value of 120 J g^{-1} [6], and w is the weight fraction of rPET in the blends or composites.

The thermal stability of the sample was analyzed by TGA on a Mettler Toledo TGA/SDTA 851^e analyzer (Switzerland) under a continuous flow of N_2 gas at a heating rate of 20°C min^{-1} over a temperature range of 100 to 800°C. The temperatures for onset (T_{onset}), end set (T_{endset}), 50% weight loss ($T_{50\%}$) and maximum decomposition rate (T_{max}) were reported.

The initial weight of each fully dried rectangular sample (5 × 12.7 × 3 mm^3) was measured, and then immersed in a water bath. The sample was periodically taken out of the bath, the water was removed from its surface by tissue paper, and then weighed. At least five specimens were weighed for each sample. The % water uptake at time, was calculated using Eq. (2),

$$\text{Water uptake } (\%) = [w_1 - w_0/ w_0] \times 100 \qquad (2)$$

where w_0 and w_1 refer to the initial weight of the dried sample and the weight of the wet sample at time, respectively.

3. Results and discussion

3.1 Mechanical properties

The effects of blend composition on the mechanical properties (impact strength, tensile strength, Young's modulus, elongation at break and flexural strength) of the rPET/PBAT blends with respect to the neat rPET are shown in Figure 1, and all the mean values with respect to both the neat rPET and PBAT are presented in Table 1. The notched Izod impact strength of each of the five different rPET/PBAT blends was higher than that of the rPET but varied with the PBAT content (Figure 1(a)), indicating an improved toughness of the rPET. The impact strength of the rPET blend at 10 wt% PBAT increased 1.2-fold over that of the neat rPET, and considerably increased 9.8-fold at 50 wt% PBAT. This influence was mainly attributed to the high flexibility of the PBAT, which had a great effect with increasing its content within the blends [6,17,20]. In contrast, the tensile properties of the rPET/PBAT blends showed a PBAT dose-dependent decrease in the tensile strength (from 1.1-fold lower at 10 wt% to 2.9-fold at 50 wt%) (Figure 1(b)) and Young's modulus (from 1.1-fold lower at 10 wt% to 2.5-fold at 50 wt%) (Figure 1(c)) but an increase in the elongation at break (from 2.6-fold higher at 10 wt% to 2.9-fold at 50 wt%) (Figure 1(d)), in relation to the neat rPET. This is a consequence of the very low tensile strength and Young's modulus and the very high elongation of PBAT [6,20]. The addition of PBAT to rPET also caused a dose-dependent decrease in the flexural strength with increasing PBAT contents (from 1.1-fold lower at 10 wt% to 2.5-fold at 50 wt%) (Figure 1(e)) due to the very low flexural strength of PBAT, and so the blend samples were bent easier under the load.

Table 1. Mechanical properties of rPET, PBAT, rPET/PBAT blends and rPET/PBAT/WF composites.

Sample	Impact strength (kJ/$m^{2\text{-}2}$)	Tensile strength (MPa)	Young's modulus (MPa)	Elongation at break (%)	Flexural strength (MPa)
rPET/PBAT(wt%/wt%)					
100/0	3.2±0.1	65.0±0.3	2226.8±54.5	2.0± 0.2	59.4±1.5
90/10	3.7±0.4	58.2±0.8	2019.6±49.8	5.3± 0.2	52.6±2.4
80/20	3.9± 0.7	47.7±0.2	1765.8±56.9	5.9±0.7	49.6±1.0
70/30	10.6±0.6	42.5±0.9	1586.3±42.0	9.4± 0.4	39.1±1.9
60/40	27.0±1.6	29.7±0.2	1192.5±23.3	12.3± 0.2	29.4±1.2
50/50	31.2±4.3	22.7±0.3	897.4±26.6	12.4± 0.2	23.7±1.4
0/100	N/B*	15.0±0.4	85.2±10.5	N/B	4.1±1.1

Table 1. (continue)

Sample	Impact strength (kJ/m^{2-2})	Tensile strength (MPa)	Young's modulus (MPa)	Elongation at break (%)	Flexural strength (MPa)
rPET/PBAT/WF(wt%/wt%/wt%)					
66.5/28.5/5	5.2±1.2	22.7±0.3	1630.0±54.7	2.4±0.2	39.9±0.6
63.0/27.0/10	4.5±0.2	36.3±1.6	1899.2±58.6	3.0±0.5	41.8±0.6
59.5/25.5/15	3.5±0.3	41.5±0.5	2241.2±64.3	3.4±0.2	52.6±2.4
56.0/24.0/20	3.2±0.4	42.5±1.6	2681.0±40.1	2.9±0.2	43.4±1.5
52.5/22.5/25	2.9±0.2	44.3±0.2	2830.7±69.7	2.6±0.1	44.3±0.7
49.0/21.0/30	2.8±0.1	45.0±0.8	3247.6±69.8	2.5±0.3	45.7±2.2

N/B*: not broken

Overall, the addition of the softer PBAT into the stiffer rPET was very effective at increasing the impact strength and elongation at break of the rPET in a PBAT dose-dependent manner, but at the expense of reducing the tensile strength, stiffness and flexural strength. In this study, the 70/30 (wt%/wt%) rPET /PBAT blend was selected for then preparing WPCs with six loadings of WF, ranging from 5-30 wt%, since this blend provided a good combination of strength, toughness, stiffness and cost.

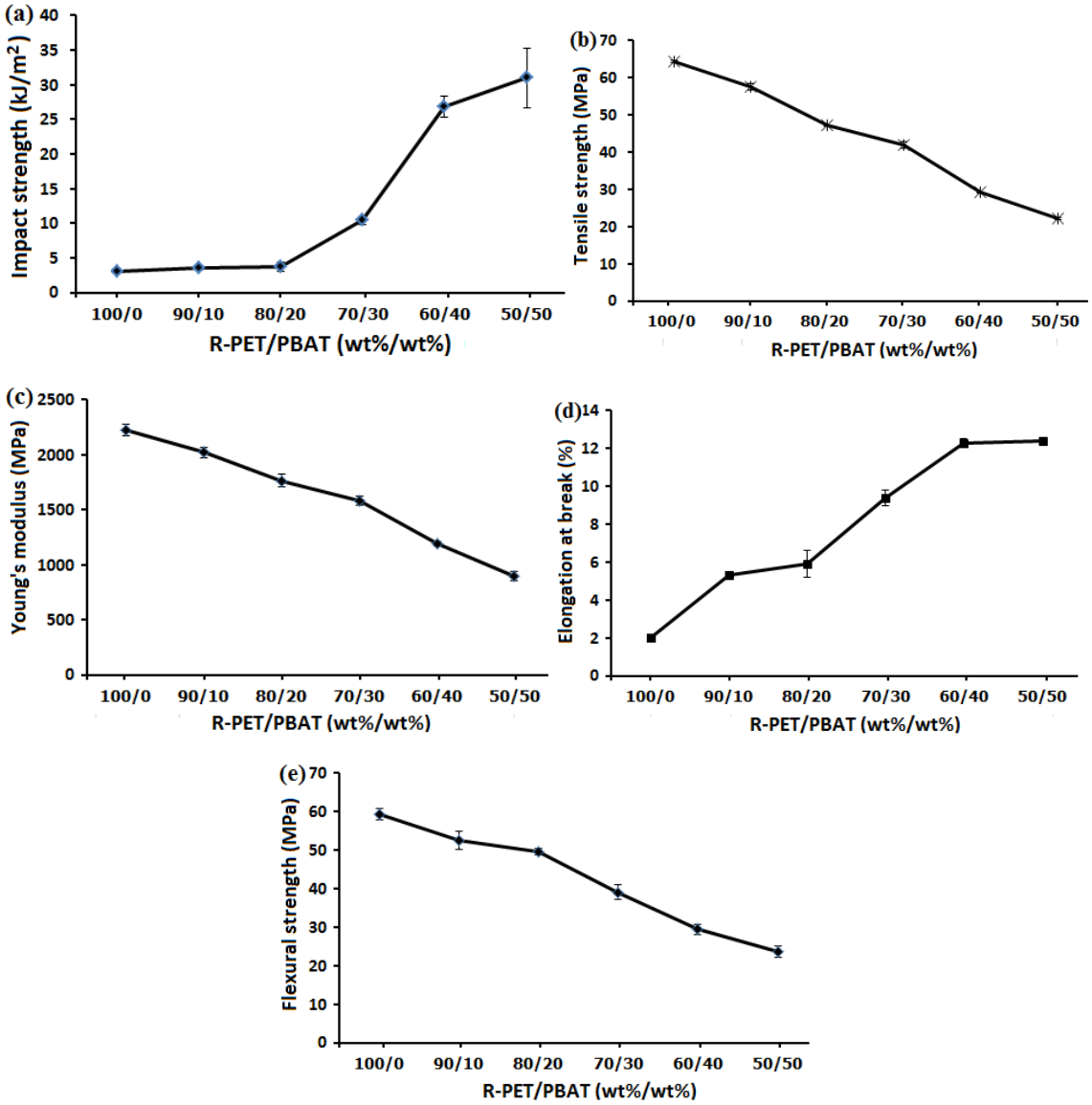

Figure 1. Mechanical properties of rPET/PBAT blends: (a) impact strength, (b) tensile strength, (c) Young's modulus (d) elongation at break and (e) flexural strength.

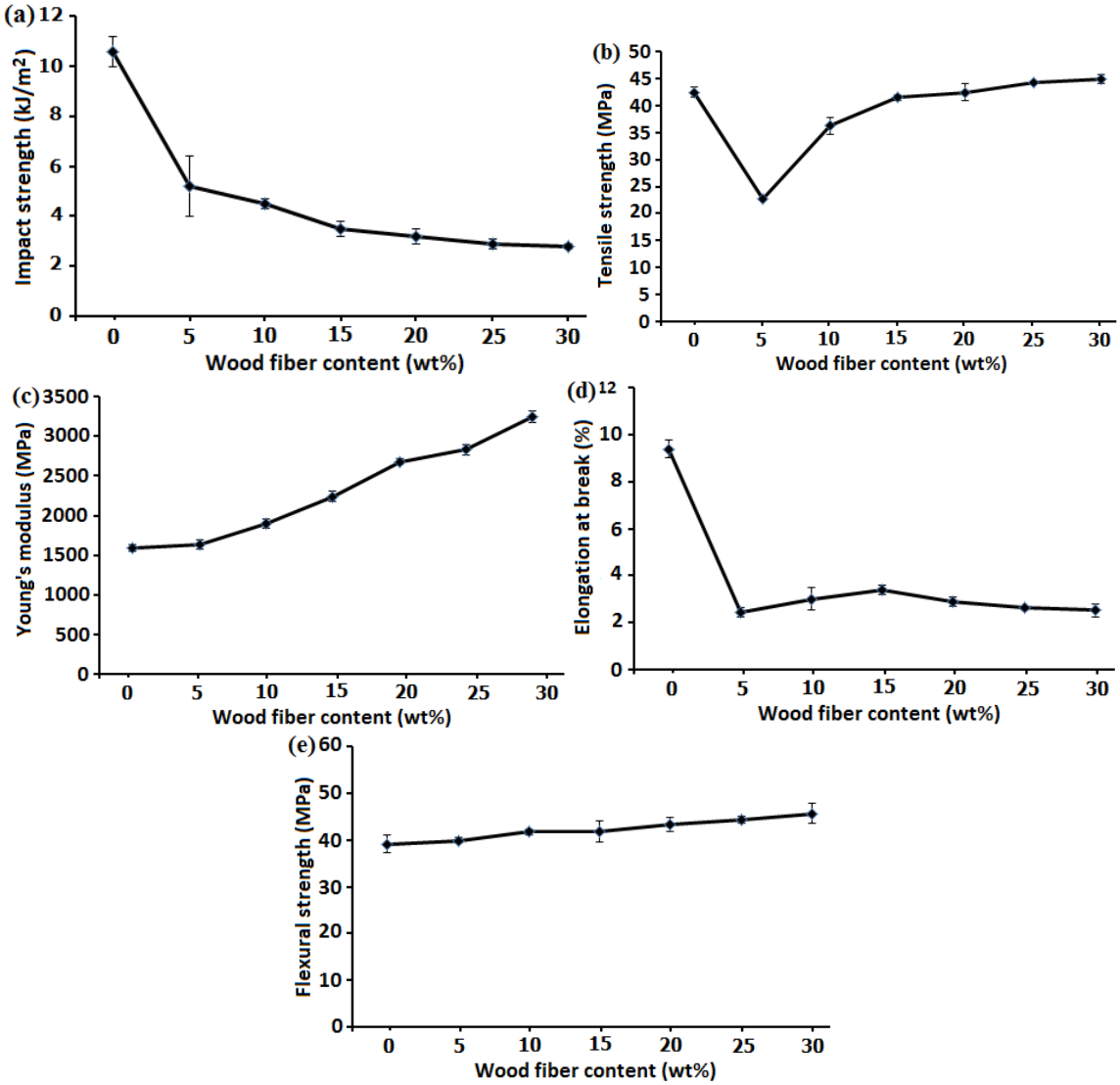

Figure 2. Mechanical properties of rPET/PBAT/WF composites: (a) impact strength, (b) tensile strength, (c) Young's modulus (d) elongation at break and (e) flexural strength.

The mechanical properties of the rPET/PBAT/WF composites are presented in Figure 2 and also given in Table 1. It is evident that the impact strength of the WPCs decreased with increasing WF contents (from 2-fold lower at 5 wt% to 3.8-fold at 30 wt%) compared to that of the 70/30 (wt%/wt%) rPET/PBAT blend (Figure 2(a)), which could be due to the high stiffness of WF particles that restricted the mobility of the polymer chains and also due to the poor polymer-WF interaction [26,27]. This indicates the less capacity to absorb energy with the addition of WF. Although all the WPCs showed a decreased impact strength with increasing WF contents, but the WPCs containing 5-20 wt% WF exhibited higher impact strength than the rPET. In contrast, the tensile strength of the WPCs (Figure 2(b)) showed an increasing trend with increasing WF contents, but the WPCs containing 5-15 wt% WF still had lower tensile strength than the 70/30 (wt%/wt%) rPET/PBAT blend (from 1.02-fold lower at 5 wt% to 1.9-fold at 15 wt%). This may be attributed to an insufficient level of WF dispersion and uniform transmission of stress in the polymer matrix. As the WF loadings increased to 20, 25 and 30 wt%, the tensile strength of the WPCs gradually increased up to a maximum value at 30 wt%, which was 1.06-fold higher than that of the neat blend. This suggests a better WF dispersion and also the orientation of WF in the WPCs in the tensile loading direction during the injection-molding process. The increase in the Young's modulus (Figure 2(c)) with increasing WF contents (from 1.03-fold higher at 5 wt% to 2-fold at 30 wt%) could be due to the high stiffness of the WF that restricted the mobility of the polymer chains. As expected, the elongation at break of the WPCs was much lower (from 2.76- to 3.92-fold) than that of the 70/30 (wt%/wt%) rPET/PBAT blend (Figure 2(d)). This was also due to the high stiffness of WF particles and the low elongation at break of WF that reduced the strain of the matrix [1]. Moreover, this probably due to the WF particle debonding from the matrix prior to

yielding as a result of the poor interfacial adhesion. However, the elongation at break of all the WPCs was still higher than that of the neat rPET. Finally, the flexural strength of the WPCs was steadily increased (Figure 2(e)) with increasing WF contents (from 1.02-fold higher at 5 wt% to 1.2-fold at 30 wt%) with respect to the neat 70/30 (wt%/wt%) rPET/PBAT blend. This enhancement could be due to the high stiffness of the WF particles that caused the WPCs to withstand the bending force. From all the above results, it is evident that the significant increase in the tensile strength, Young's modulus and flexural strength was achieved only at the high loadings of WF in the WPCs.

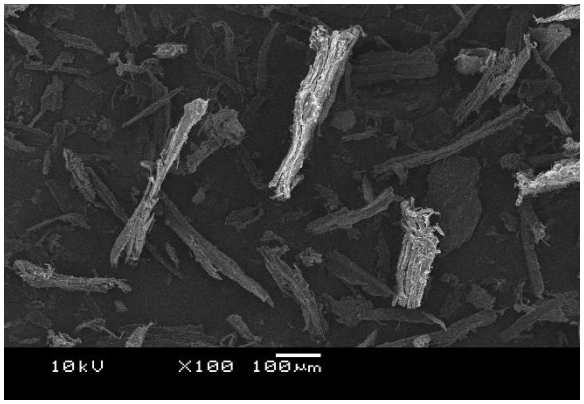

Figure 3. Representative SEM image (×100 magnification) of WF particles.

3.2 Morphology

The morphology of the WF particles observed by the SEM analysis is shown in Figure 3. The *L*/*D* of the WF particles was about 5-15. The morphology of the impact fractured surfaces of the injection-molded specimens is shown in Figures 4 and 5. The rPET showed a flat and smooth fractured surface contributing to a brittle failure behavior (Figure 4(a)), while the fractured surface of all the rPET/PBAT blends was rough with some low ridges and tear lines (Figures 4(b-f)), suggesting that the samples became more ductile. This could be due to the high flexibility of PBAT that toughened the blends. In contrast, the fractured surface of the WPCs (Figure 5) was smoother and had more voids attributed to the detachment of the WF particles from the matrix as compared to the neat 70/30 (wt%/wt%) rPET/PBAT blend, suggesting that the composites became more brittle, which is in agreement with the results of the impact strength as previously mentioned.

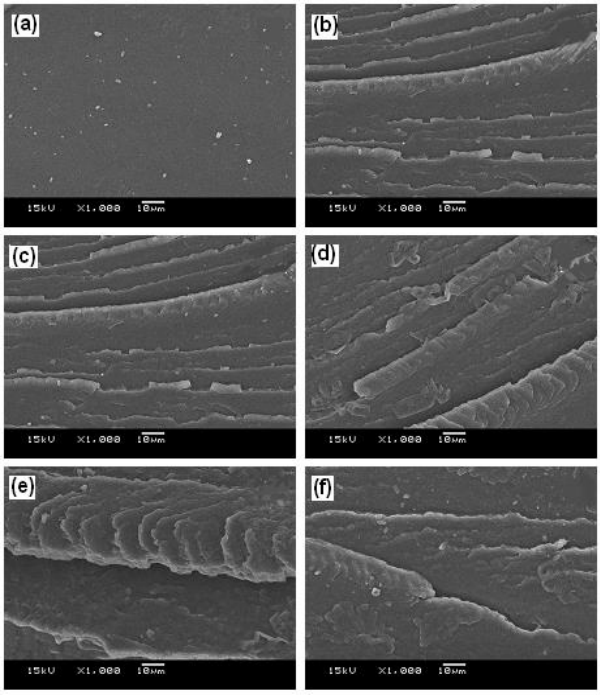

Figure 4. Representative SEM images (×1,000 magnification) of (a) rPET, (b-f) rPET/PBAT blends with PBAT at (b) 10 wt%, (c) 20 wt%, (d) 30 wt%, (e) 40 wt% and (f) 50 wt%.

Table 2. DSC-derived data of rPET, rPET/PBAT blends and rPET/PBAT/WF composites.

Sample	Cooling run	Second heating run			
	T_c (°C)	T_{m1} (°C)	T_{m2} (°C)	ΔH_m (J g^{-1})	$\chi_{c,\,rPET}$ (%)
rPET/PBAT(wt%/wt%)					
100/0	200.6	242.3	247.8	41.0	34.2
90/10	191.2	234.7	245.0	36.2	33.5
80/20	177.1	221.2	-	24.5	25.5
70/30	163.4	209.3	-	20.6	24.5
60/40	146.5	192.6	-	18.2	25.3
50/50	143.5	185.8	-	16.1	26.8
rPET/PBAT/WF(wt%/wt%/wt%)					
66.5/28.5/5	204.5	235.5	248.0	26.6	33.3
63.0/27.0/10	204.3	235.0	247.8	36.4	48.1
59.5/25.5/15	203 .3	235.0	246.6	31.4	44.0
56.0/24.0/20	201.0	233.5	245.4	30.6	45.5
52.5/22.5/25	199.8	232.0	245.5	24.3	38.6
49.0/21.0/30	199.6	230.5	240.0	26.7	45.4

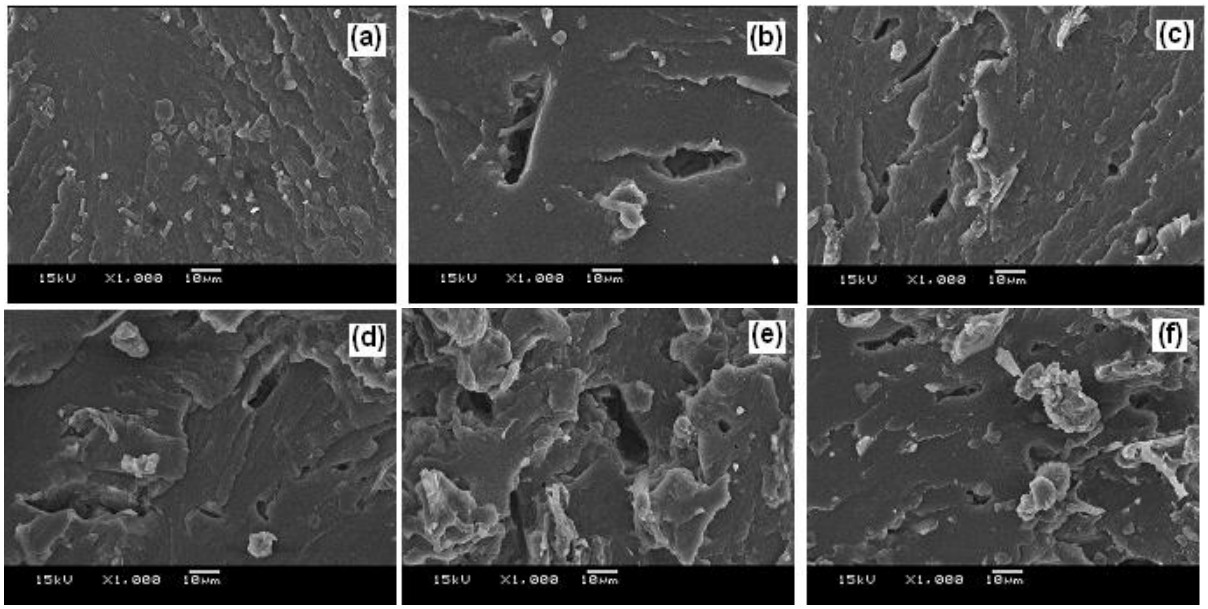

Figure 5. Representative SEM images (× 1,000 magnification) of the 70/30 rPET/PBAT blend composites with WF at (a) 5 wt%, (b) 10 wt%, (c) 15 wt%, (d) 20 wt%, (c) 25 wt% and (f) 30 wt%.

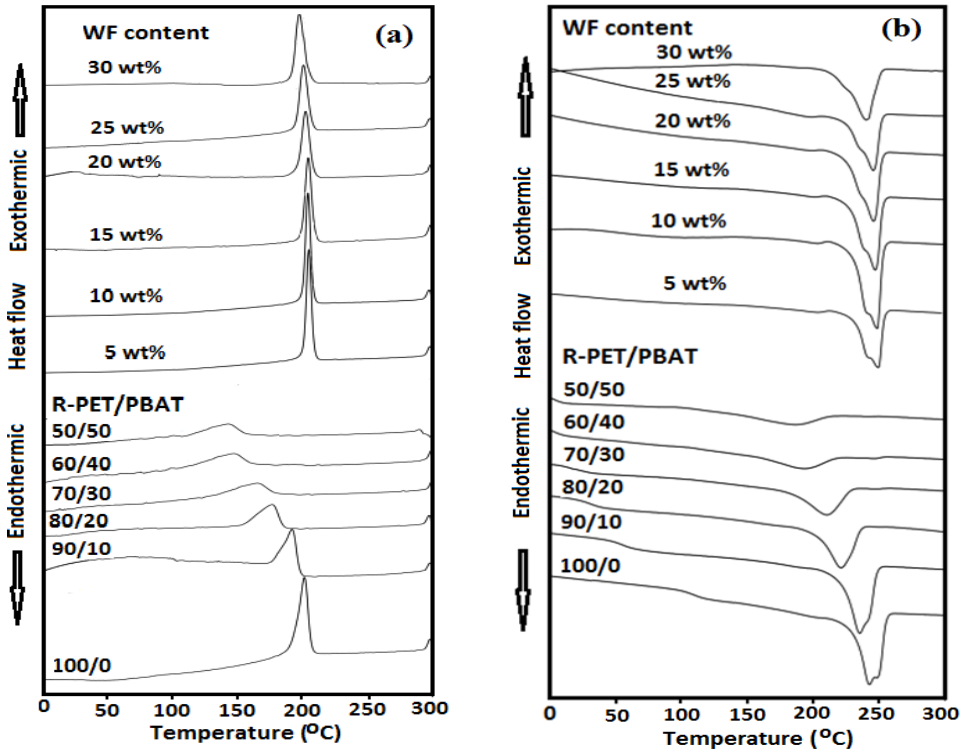

Figure 6. DSC thermograms of rPET, rPET/PBAT blends and rPET/PBAT/WF composites obtained during the (a) cooling and (b) second heating scans.

3.3 Thermal properties

Representative DSC thermograms of the samples obtained from the cooling and second heating scans are shown in Figure 6, and the corresponding crystallization and melting behaviors (T_c, T_m, ΔH_m and χ_c) are summarized in Table 2. A single exothermic peak in each of the cooling DSC curve (Figure 6(a)) corresponds to the crystallization of rPET after erasing the thermal history during the first heating scan. The T_c of rPET was about 200.6°C, indicating a sufficient time for the rPET to crystallize during the cooling scan at 10°C min^{-1}. The addition of PBAT (10-50 wt%) to rPET caused a dose-dependent reduction in the T_c of the rPET component in all the rPET/PBAT blends by 9.4-63.1°C, reflecting a longer time for rPET to crystallize, which was due to the restricted arrangement or orientation of the rPET chains by

PBAT molecules. In contrast, the T_c of rPET in all the WPCs was higher (36.2-41.1°C) than that of the 70/30 (wt%/wt%) rPET /PBAT blend, suggesting that the dispersed WF particles accelerated the crystallization of rPET by acting as a nucleating agent during the cooling scan [25].

The second heating scan displayed double melting endothermic peaks of the rPET at 242.3°C (T_{m1}) and 247.8°C (T_{m2}) (Figure 6(b)). The first peak corresponds to the melting of the less perfect or smaller crystals formed during the cooling scan, while the second peak corresponded to the melting of the higher structural perfection crystals formed through recrystallization and reorganization during the second heating scan [28,29]. The inclusion of 10 wt% PBAT into rPET caused a decrease in the T_{m1} and T_{m2} of the rPET component by 7.6 and 2.8°C, respectively, due to the very low T_m of PBAT (~120°C). The rPET/PBAT blends containing 20-50 wt% PBAT exhibited merely one melting endotherm due to the restriction of the rPET recrystallization from the high loading level of PBAT. After the addition of WF to the 70/30 (wt%/wt%) rPET/PBAT blend, the obtained composites again showed double melting peaks or small shoulder peaks (230.5-235.5°C for T_{m1} and 240-248°C for T_{m2}), which were all higher than those of the 70/30 (wt%/wt%) rPET/PBAT blend. In addition, the χ_c of the rPET component in all the rPET/PBAT blends was lower than that of the neat rPET, indicating that the PBAT molecules restricted the arrangement or orientation of the rPET chains. However, the χ_c of the rPET component in the WPCs was much higher than that of the 70/30 (wt%/wt%) rPET/PBAT blend, suggesting that the WF particles facilitated the rPET crystallization.

Representative TG and derivative thermogravimetric (DTG) thermograms of the samples are shown in Figures 7 and 8. The T_{onset}, T_{endset}, $T_{50\%}$ and T_{max} obtained from the TG/DTG curves of all the samples are summarized in Table 3. The thermal decomposition of either rPET or PBAT generally takes place via the breakdown of ester groups and chain scission of C-O and C-C bonds on the polymer backbones. From Figure 7, all the rPET/PBAT blends exhibited one stage decomposition and a similar characteristic just like the rPET, but had lower decomposition temperatures. The continuous decrease in the thermal stability of the blends as PBAT content increased was attributed to the lower thermal stability of the PBAT compared to that of the rPET. As can be seen, the TG curves of all the rPET/PBAT/WF composites exhibited two decomposition steps (Figure 8(a)), where the first step in the range of 270.5-401.1°C was related to the decomposition of WF, and the second step in the range of 380-460.4°C was attributed to the decomposition of the polymer matrix [22]. Moreover, the T_{max} of the WF in all the WPCs could be observed from the shoulder in the DTG curves (Figure 8(b)), which was in the range of 364.1-370.4°C, while the T_{max} of the matrix occurred within the range of 424.4-432.4°C. Because WF has lower thermal stability than the rPET and PBAT, the thermal stability of the WPCs continuously decreased with increasing WF loading levels compared to that of the 70/30 (wt%/wt%) rPET/PBAT blend.

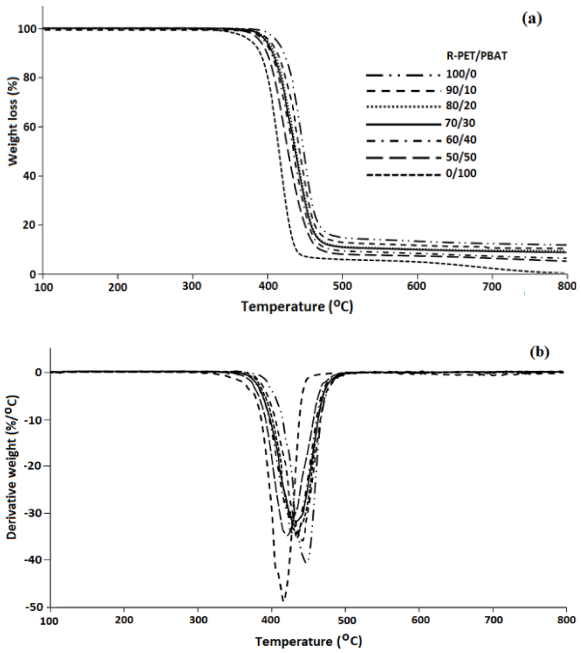

Figure 7. (a) TG and (b) DTG thermograms of rPET, PBAT and rPET/PBAT blends.

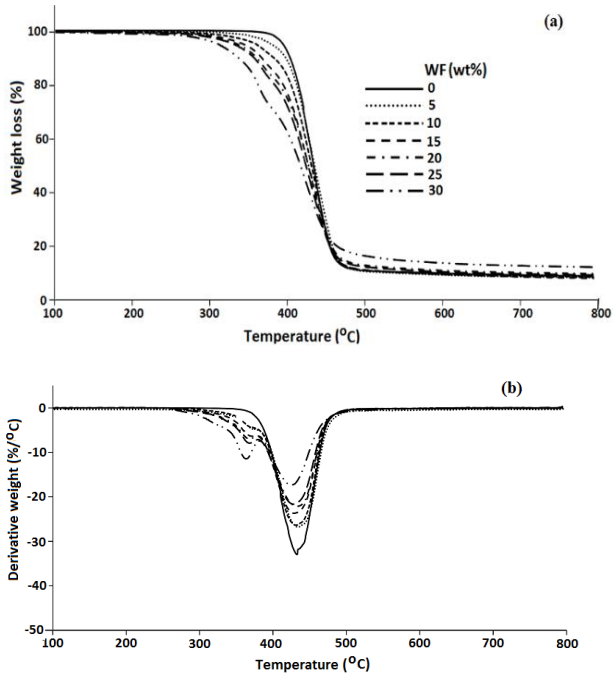

Figure 8. (a) TG and (b) DTG thermograms of 70/30 (wt%/wt%) rPET/PBAT blend and its composites with WF.

Table 3 Thermal stability of rPET, PBAT, WF, rPET/PBAT blends and rPET/PBAT/WF composites

Sample	$T_{onset\ 1}$ (°C)	$T_{endset\ 1}$ (°C)	$T_{max\ 1}$ (°C)	$T_{onset\ 2}$ (°C)	$T_{endset\ 2}$ (°C)	$T_{max\ 2}$ (°C)	$T_{50\%}$ (°C)
WF	270.0	400.0	375.0	-	-	-	370.5
rPET/PBAT(wt%/wt%)							
100/0	420.5	463.5	447.3	-	-	-	446.1
90/10	413.7	462.9	442.3	-	-	-	440.8
80/20	405.0	462.0	434.4	-	-	-	436.2
70/30	404.1	461.7	433.6	-	-	-	435.8
60/40	402.4	456.2	430.7	-	-	-	432.3
50/50	396.8	449.6	422.1	-	-	-	425.2
0/100	391.3	432.1	416.0	-	-	-	413.2
rPET/PBAT/WF(wt%/wt%/wt%)							
66.5/28.5/5	320.4	401.1	370.4	401.2	460.4	432.4	435.6
63.0/27.0/10	300.6	394.6	370.0	395.0	459.8	431.9	431.9
59.5/25.5/15	290.3	386.7	370.0	387.0	459.2	429.5	427.8
56.0/24.0/20	282.7	384.8	369.1	385.0	458.0	429.1	428.1
52.5/22.5/25	280.2	384.0	368.9	385.0	457.5	428.6	424.9
49.0/21.0/30	270.5	379.6	364.1	380.0	455.5	424.4	417.9

3.4 Water uptake

Figure 9 shows the percentage of water uptake of the rPET, PBAT, rPET/PBAT blends and rPET/PBAT/WF composites at different periods of immersion (0-30 days). Initially, the water uptake of all the samples increased rapidly, followed by a slower absorption until reaching a saturated point, which less water was absorbed and the water content in the samples approached a constant value over the period of 30 days. From Figure 9(a), the water uptake of the rPET was lower than that of the PBAT, due to the higher hydrophobicity of the rPET. The maximum water uptake of the rPET and PBAT was about 0.63 and 0.96%, respectively. As a consequence, the water uptake of the rPET/PBAT blends increased with increasing PBAT contents compared to that of the rPET, due to the higher water uptake of PBAT and the space between the rPET and PBAT molecules that facilitated the water absorption. Thus, the maximum water uptake of the rPET/PBAT blends increased continuously from 0.68% at 10 wt% PBAT to 0.87% at 50 wt% PBAT. Figure 9(b) shows the effect of WF on the water uptake of the WPCs over the same period of time (30 days). Generally, the water uptake increased with WF loading because of an increased free hydroxyl groups (OH), which interacted with water molecules through hydrogen bonding, leading to the weight gain of the WPCs [23]. Therefore, the water uptake of WPCs increased steadily with increasing WF loadings compared to that of the 70/30 (wt%/wt%) rPET/PBAT blend. Moreover, the space at the interphase between the hydrophilic WF and the hydrophobic polymer matrix also caused an increase in the water uptake of the WPCs, and so the maximum water uptake of the WPCs increased steadily from 1.38% at 5 wt% WF to 4.4% at 30 wt% WF. This suggests that the WPCs has strong tendency to degrade by allowing the microorganism to penetrate into the products using water as a medium.

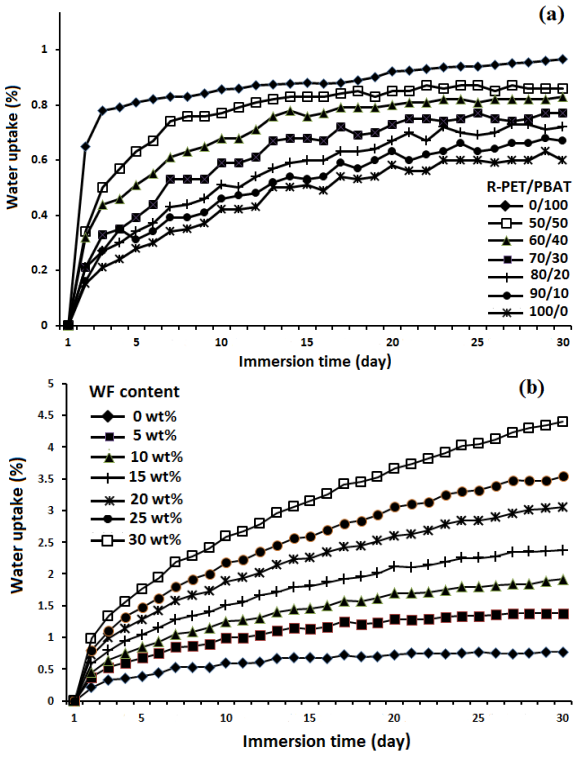

Figure 9 Water uptake of (a) rPET and rPET /PBAT blends and (b) rPET/PBAT/WF composites.

4. Conclusions

PBAT-toughened rPET blends were successfully prepared by melt processing. The impact strength and elongation at break of the blends were found to be improved as a function of composition, while the tensile strength, Young's modulus and flexural strength were deteriorated. It was found that the 70/30 (wt%/wt%) rPET/PBAT blend exhibited a sign of brittle-to-ductile transition and also a good combination of strength, toughness, stiffness and cost.

This blend was then selected for preparing WPCs with six loadings of WF (5-30 wt%) in order to solve the environmental issue by increasing their biodegradability after discarding. It is also noticed that all the WPCs had lower impact strength and elongation at break than the neat blend. However, the WPCs with 5-15 wt% WF had higher impact strength than the rPET (optimal at 5 wt% WF), while all the WPCs had higher elongation at break than the rPET (optimal at 15 wt% WF). Moreover, the tensile strength, Young's modulus and flexural strength of the WPCs exhibited different trends. As can be seen, the tensile strength of the WPCs was improved only at 25 and 30 wt% WF (optimal at 30 wt% WF), while the Young's modulus and flexural strength of the WPCs were all enhanced (optimal at 30 and 15 wt% WF, respectively) compared with those of the neat blend. However, the Young's modulus of the WPCs at 5 and 10 wt% WF as well as the flexural strength of all the WPCs were lower than those of the rPET. In addition, the DSC and TGA analysis revealed an increase in the T_c, the T_m and the χ_c, but a decrease in the thermal stability of the WPCs, respectively, with increasing WF contents compared to those of the neat blend. The maximum water uptake of the WPCs was also found to be increased with increasing WF contents. Hence, the prepared WPCs with proper compositions may regain the performance of the rPET as an environmentally friendly material.

5. Acknowledgments

The authors would like to acknowledge MTEC, National Science and Technology Development Agency (NSTDA), Department of Materials Science and Department of Petrochemical and Polymer Science, Faculty of Science, Chulalongkorn University for financial, material and instrument support.

References

[1] S. K. Najafi, "Use of recycled plastics in wood plastic composites-A review", Waste Management, vol. 33, pp. 1898-1905, 2013.

[2] S. K. Najafi, M. M. Marznaki and M. Chaharmahali, "Effect of thermomechanical degradation of polypropylene on mechanical properties of wood-polypropylene composites", Journal of Composite Materials, vol. 43, pp. 2543-2555, 2009.

[3] A. Ashori and A. Nourbakhsh, "Characteristics of wood-fiber plastic composites made of recycled materials", Waste Management, vol. 29, pp. 1291-1295, 2009.

[4] T. Huq, A. Khan, T. Akter, N. Noor, and K. Dey, "Thermo-mechanical, degradation, and interfacial properties of jute fiber-reinforced PET-based composite", Journal of Thermoplastic and Composite Materials, vol. 24, pp. 889-898, 2011.

[5] Y. Zong, Y. Cheng and G..Dai, "The relationship between rheological behavior and toughening mechanism of toughened poly(ethylene terephthalate). Journal of Composite Materials vol. 42, pp. 1571-1585, 2008.

[6] Y. Srithep, A. Javadi, S. Pilla, L.S. Turng, S. Gong, C. Clemons, J. Peng, "Processing and characterization of recycled poly(ethylene terephthalate) blends with chain extenders, thermoplastic elastomer, and/or poly(butylene adipate-co-terephthalate)", Polymer Engineering and Science, vol. 51, pp. 1023-1032, 2011.

[7] N.M. Abdullah and I. Ahmad, "Potential of using reinforced coconut fiber composites derived from recycling polyethylene terephthalate (PET) waste", Fibers and Polymers, vol. 14, pp. 584-590, 2013.

[8] H. Nabil, H. Ismail and A.R. Azura, "Recycled polyethylene terephthalate filled natural rubber compounds: effects of filler loading and types of matrix", Journal of Elastomers and Plastics, vol. 43, pp. 429-449, 2011.

[9] Y. Zhang, H. Zhang, L. Ni, et al. Crystallization and mechanical properties of recycled poly(ethylene terephthalate) toughened by styrene-ethylene/butylene-styrene elastomer", Journal of Polymers and the Environment, vol. 18, pp. 647-653, 2010.

[10] N. Kerboua, N. Cinausero, T. Sadoun and J.M. Lopeze-Cuesta, "Effect of organoclay in an immiscible poly(ethylene terephthalate) waste/ poly (methyl methacrylate) blend", Journal of Applied Polymer Science", vol. 117, pp. 129-137, 2010.

[11] S. Mbarek and M. Jaziri, "Recycling poly (ethylene terephthalate) wastes: properties of poly(ethylene terephthalate)/polycarbonate blends and the effect of a transesterification catalyst", Polymer Engineering and Science, vol. 46, pp. 1378-1386, 2006.

[12] P. Phinyocheep, J. Saelao and J.Y. Buzaré, "Mechanical properties, morphology and molecular characteristics of poly(ethylene terephthalate) toughened by natural rubber", Polymer, vol. 48, pp. 5702-5712, 2007.

[13] K. Oksman, M. Skrifvars and J.F. Selin, "Natural fibres as reinforcement in polylactic acid (PLA) composites", Composite Science and Technology, vol. 63, pp. 1317-1324, 2013.

[14] E. Petinakis, L. Yu, G. Edward, K. Dean, H. Liu and A.D. Scully, "Effect of matrix-particle interfacial adhesion on the mechanical properties of poly(lactic acid)/wood-flour micro-composites.", Journal of Polymers and the Environment, vol. 17, pp. 83-94, 2009.

[15] Y.J. Phua, W.S. Chow and Z.A. Mohd Ishak, "Poly(butylene succinate)/organo-montmorillonite nanocomposites: effects of the organoclay

content on mechanical, thermal, and moisture absorption properties", Journal of Thermoplastic and Composite Materials, vol. 24, pp. 133-151, 2011.

[16] R.A. Khan, A.J Parsons, I.A. Jones, G.S. Walkers and C.D. Rudd, "Effectiveness of 3-aminopropyl-triethoxy-silane as a coupling agent for phosphate glass fiber-reinforced poly(caprolactone)-based composites for fracture fixation devices", Journal of Thermoplastic and Composite Materials, vol. 24, pp. 517-534, 2011.

[17] A.S. Hadj-Hamou, S.Matssi, H. Abderrahmane and F. Yahiaoui, "Effect of cloisite 30B on the thermal and tensile behavior of poly(butylene adipate-co-terephthalate)/poly(vinyl chloride) nanoblends", Polymer Bulletin, vol. 71, pp. 1483-1503, 2014.

[18] N.R. Savadekar, P.G. Kadam and S.T. Mhaske, "Studies on the effect of nano-alumina on the performance properties of poly(butylene adipate-co-terephthalate) composite films", Journal of Thermoplastic and Composite Material, vol. 28, pp. 1522-1536, 2015.

[19] X. Zhou, A. Mohanty and M. Misra, "A new biodegradable injection moulded bioplastic from modified soy meal and poly(butylene adipate-co-terephthalate: effect of plasticizer and denaturant", Journal of Polymers and the Environment, vol. 21, pp. 615-622, 2013.

[20] S. Chuayjuljit, P. Chaiwutthinan, L. Raksaksri and A. Boonmahitthisud, "Effects of poly(butylene adipate-co-terephthalate) and ultrafined wollastonite on the physical properties and crystallization of recycled poly(ethylene terephthalate)", Journal of Vinyl & Additives Technology, vol. 23, pp. 106-116, 2017.

[21] B. Kord, D.T. Haratbar, B. Malekian and S. Ismaeilimoghadam, "Effect of chemical modification of wood flour on long-term hygroscopic behavior of polypropylene composites", Journal of Thermoplastic and Composite Materials, vol. 2, pp. 577-588, 2016.

[22] Y. Karaduman and L. Onal, "Dynamaic mechanical and thermal properties of enzyme-treated jute/ polyester composites", Journal of Composite Materials, vol. 47, pp. 2361-2370, 2012.

[23] C. Homkhiew, T. Ratanawilai and W. Thongruang, "Long-term water absorption and dimensional stability of composites from recycled polypropylene and rubberwood flour", Journal of Thermoplastic and Composite Material, vol. 29, pp. 74-91, 2014.

[24] M. Poletto, M. Zeni and A. Zattera, "Effect of wood flour addition and coupling agent content on mechanical properties of recycled polystyrene/wood flour composites", Journal of Thermoplastic and Composite Material, vol. 25, pp. 821-833, 2011.

[25] D. Ndiaye and A.Tidjani, "Effects of coupling agents on thermal behavior and mechanical properties of wood flour/polypropylene composites", Journal of Composite Materials, vol. 46, pp. 3067-3075, 2012.

[26] S. Chuayjuljit, C. Wongwaiwattanakul, P. Chaiwutthinan and P. Prasassarakich, "Biodegradable poly(lactic acid)/poly(butylene succinate)/wood flour composites: physical and morphological properties", Polymer Composites, vol. 38, pp. 2841-2851, 2017.

[27] S. Chuayjuljit, J. Kongthan, P. Chaiwutthinan, and A. Boonmahitthisud, "Poly(vinyl chloride)/ poly(butylene succinate)/wood flour composites: physical properties and biodegradability", Polymer Composites, vol. 39, pp. 1543-1552, 2017.

[28] J. Dou and Z. Liu, "Crystallization behavior of poly(ethylene terephthalate)/ pyrrolidinium ionic liquid", Polymer International, vol. 62, pp. 1698-1710, 2013.

[29] A.M. Diez-Pascual and A.L. Diez-Vicente, "Poly(3-hydroxybutyrate)/ZnO bionanocomposites with improved mechanical, barrier and antibacterial properties", International Journal of Molecular Science, vol. 15, pp. 10950-10973, 2014.